remote sensing

MDPI

Article

Analysis of Settlement Expansion and Urban Growth Modelling Using Geoinformation for Assessing Potential Impacts of Urbanization on Climate in Abuja City, Nigeria

Mahmoud Ibrahim Mahmoud [1,2,*], Alfred Duker [3], Christopher Conrad [2], Michael Thiel [2,*] and Halilu Shaba Ahmad [4]

1 College of Engineering, Civil Engineering Department, Graduate Research Programme in Climate Change and Land Use, Kwame Nkrumah University of Science and Technology, University Post Office Box PMB, Kumasi, Ghana
2 Institute of Geography and Geology, University of Würzburg, Oswald-Külpe-Weg 86, 97074 Würzburg, Germany; christopher.conrad@uni-wuerzburg.de
3 College of Engineering, Geometrics Engineering Department, Kwame Nkrumah University of Science and Technology, University Post Office Box PMB, Kumasi, Ghana; duker@alumni.itc.nl
4 National Space Research and Development Agency (NASRDA), Obasanjo Space Center, Airport Road, PMB 437, Garki, Abuja, Nigeria; drhalilu@yahoo.com
* Correspondence: salammahmoudiii@gmail.com (M.I.M.); michael.thiel@uni-wuerzburg.de (M.T.); Tel.: +233-261-306-742 (M.I.M.)

Academic Editors: Parth Sarathi Roy and Prasad S. Thenkabail
Received: 11 January 2016; Accepted: 4 March 2016; Published: 9 March 2016

Abstract: This study analyzed the spatiotemporal pattern of settlement expansion in Abuja, Nigeria, one of West Africa's fastest developing cities, using geoinformation and ancillary datasets. Three epochs of Land-use Land-cover (LULC) maps for 1986, 2001 and 2014 were derived from Landsat images using support vector machines (SVM). Accuracy assessment (AA) of the LULC maps based on the pixel count resulted in overall accuracy of 82%, 92% and 92%, while the AA derived from the error adjusted area (EAA) method stood at 69%, 91% and 91% for 1986, 2001 and 2014, respectively. Two major techniques for detecting changes in the LULC epochs involved the use of binary maps as well as a post-classification comparison approach. Quantitative spatiotemporal analysis was conducted to detect LULC changes with specific focus on the settlement development pattern of Abuja, the federal capital city (FCC) of Nigeria. Logical transitions to the urban category were modelled for predicting future scenarios for the year 2050 using the embedded land change modeler (LCM) in the IDRISI package. Based on the EAA, the result showed that urban areas increased by more than 11% between 1986 and 2001. In contrast, this value rose to 17% between 2001 and 2014. The LCM model projected LULC changes that showed a growing trend in settlement expansion, which might take over allotted spaces for green areas and agricultural land if stringent development policies and enforcement measures are not implemented. In conclusion, integrating geospatial technologies with ancillary datasets offered improved understanding of how urbanization processes such as increased imperviousness of such a magnitude could influence the urban microclimate through the alteration of natural land surface temperature. Urban expansion could also lead to increased surface runoff as well as changes in drainage geography leading to urban floods.

Keywords: land-cover change; settlement expansion; support vector machines; urban growth modelling; climate impact

1. Introduction

Some of the most dynamic places on planet Earth are urbanized locations developing across multiple dimensions. Globally, the expansion of urban forms is documented to be a principal front in habitat destruction which begins with habitat loss and later results in species extinction [1]. Notwithstanding their importance, their growth is associated with huge impacts on contiguous ecosystems [2]. For instance, the loss of arable agricultural land to urbanization, especially in developing nations, is flagged to be a result of prevalent anthropogenic activities [3,4]. Similarly, the unprecedented transformation of natural landscapes into urban settings significantly affects the natural functioning of ecosystems [5]. Hence, urbanization has been the foremost human led land-use anthropogenic activity with huge and irreversible impacts. It is a major force that drives changes such as land-use land-cover change (LULCC), biodiversity loss, the biogeochemical cycle, hydrological systems and climate [6]. Another prominent agent that can be linked to the unprecedented growth witnessed in urban expansion is population increase [7]. One hundred years ago, of every 10 persons, two resided in urban areas. By 2030, the number of people living in urban areas is likely to hit six, and by 2050 seven out of every 10 [8]. Since the 1950s, the number of global urban inhabitants has increased, and by 2050 a two fold increase is anticipated from an approximate value of 3.4 thousands of million as of 2009 to 6.4 thousands of million by 2050 [8]. The year 2020 is projected to be when the majority of mega cities in the world will be in developing countries due to differential population growth and anthropogenic activities such as change in LULC [9,10]. Therefore, governments in West African countries and Nigeria in particular must act fast to better understand spatial and urban growth patterns for improved municipal planning.

The pathway to understanding the process of urbanization can be established by deliberate monitoring of biophysical and socioeconomic conditions of the existing and transformed urban areas [11]. However, reliable information on the biophysical dimensions of urban landscapes, especially the urban LULC of the built environment, can be difficult to obtain. Hence, remotely sensed data and its applications can provide critical information about urbanization in order to advance urban science for improved policy and decision making. However, having access to requisite biophysical, socio-economic characteristics of the urban areas is difficult because gaps exist between these data streams. Moreover, linkages between data collection time lags, administrative and landscape units and spatio-temporal scales pose great challenges.

A paucity of reliable information has coincided with a period when substantial growth in urban areas has been witnessed worldwide, and hopes are high among policy makers and research groups that this information gap can be filled. These groups hope that fine-scale information will be increasingly made available to comprehend the impacts of urbanization on local environments and human security such as temperature variability linked to urban heat and cold islands and local environmental and climate change/variability. This has paved the way lately for more attention being directed towards urbanization science with new directions in data collection and analysis [12], as well as monitoring changes in urban LULC considering its strong influence on ecosystems [13]. Remarkably, remote sensing scientists are responding to the call for linked environmental and socio-economic information through the advancement of remotely sensed data application and methods [14–17].

The support vector machine (SVM) method is one of the latest additions to the existing catalogue of superior and robust image classification techniques for handling multispectral satellite images that support LULC analysis, considering their non-linearity and multidimensionality [18–20]. The SVM-based approach is a non-parametric machine learning algorithm that uses hyperplanes to separate features of different categories with a maximum distance margin located close to it [21]. The best generalization is achieved when the margin distance is farthest from vectors from both classes despite minimal training samples which previously limited numerous remote sensing applications [19].

One of the standard ways of simplifying reality is the use of models and, in spatial analysis, LULCC mapping, monitoring and modelling can be regarded as models used for decision support to assess the root causes and implications. Modelling LULCC leads to improved understanding of human–environmental systems' interaction toward sustainable and spatially framed land-use policy

development and planning [22,23]. Hence, such spatial models are suitable for assessing arrays of complex biophysical and socioeconomic drivers of spatiotemporal patterns of LULCC and measuring the change consequences [24]. Lately, different models such as the cellular automata-based, agent-based, machine learning, and spatially explicit approaches have been applied to study changes in LULC [25–27]. Similarly, the land change modeler (LCM) has been used to model urban sprawl and growth [28,29]. Hua *et al* [30] ran the SELUTH model which derives its name from input data requirements to run the model slope, land use, exclusion, urban extent, transportation and hill shade over Jimei in Fujian Province, China. Other approaches such as artificial neural networks have also been applied for urban modeling studies [31–33]. The LCM approach is embedded in the IDRISI package which is an integrated environment suitable for analysis, prediction and validation of LULCC [34]. LCM uses categorical gridded images with the same land-cover types sequentially similar in order of arrangement as input for modelling LULCC [35]. Land-cover changes are evaluated across multiple time lines, and change results are calculated and presented in the form of graphs and maps. The subsequent step is predicting the future by generating LULC maps based on the transition potential maps [35], trusting the Multi-Layer Perception (MLP) neural networks output [36]. For short time frames, the LCM performed better with good prediction accuracies particularly with stable land-covers types against rapid conversion [35]. Also, comparing LCM outputs to other LULCC models that predict change based on supervised classifiers such as the weights of evidence (WoE) approach that uses user defined weighting, more accurate change maps are generated. This is because the final change map uses the overall change potential maps which are based on neural network outputs that are capable of expressing changes in various land-cover types much better than single probabilities derived from the WoE approach [36].

The federal capital territory (FCT) of Nigeria was established in 1976 but physical development only began in 1980 [37], and it has been characterized as one of the fastest growing cities in West Africa [38]. The territory has experienced rapid LULC changes, urban spatial expansion and transportation infrastructure expansion over the last 30 years and is the major focus of urban spatial analysis in this study. Over time, urban growth significantly changed in Abuja which gave way to complex urban dynamics such as conversion of agricultural land to settlement, road and infrastructure [37], population growth with an estimated annual growth rate of 9.4% [39]. Table 1 presents an overview of how significant population growth in the federal capital city (FCC) differs from other parts of the FCT, which indicates that rapid population growth is a major driver to consider in this study. For instance, the decrease in agricultural activities and concomitant loss of cultivated land is likely to contribute to landlessness and food shortages and put the livelihood of inhabitants in jeopardy. To date, obtaining information on the environmental and socio-economic sustainability of Abuja, which is essential for development planning, has received relatively little attention. So far, no available systematic study of the spatiotemporal dynamics of urban growth changes in Abuja in the context of climate impacts has been conducted. In terms of short, medium and long-term development, this current study is appropriate to bridge the knowledge lacuna between these urban events. One of the few studies that has previously been conducted was detecting Land-use Land-cover change (LULCC) in Abuja and that was based on the maximum likelihood classifier [40].

Table 1. Population statistics of the municipalities in FCT for the year 2006.

Municipality Name	No of Inhabitants Population	No of Households Units
Abuja Municipal (AMAC)	776,298	188,093
Abaji	58,642	10,572
Bwari	229,274	51,797
Gwagwalada	158,618	33,196
Kuje	97,233	17,696
Kwali	86,174	15,206
Total	1,406,239	316,560
Mean	234,373.2	52760

This study aims to integrate remotely sensed and ancillary data such as a master plan, digital elevation model and the population to detect LULCC from 1984 to 2014, and spatiotemporally analyze the settlement expansion pattern and model changes to project the LULC in 2050 using LCM in the context of climate impact. Major themes considered to achieve the goal of this study included biophysical information extracted from remotely sensed data as a baseline for subsequent applications such as analyzing settlement expansion which is the focus of this work. Other aspects investigated are the development of a land use change index and modelling urban growth (from the past into the future using LCM which can be contextualized for potential climate change impacts). The subsequent subsection presents and describes the study area considering the anthropogenic land-use situation and potential climate change impacts.

2. Material and Methods

2.1. Study Area

The study area (Figure 1), also known as the FCC, falls within the FCT occupying approximately 400 km^2. It is located in the center of Nigeria between 7°20′ and 9°15′ North of the Equator and longitudes 6°45′ and 7°39′ East. In the tropics under the Köppen climate classification, Abuja features a tropical wet and dry climate thereby experiencing three weather conditions annually. This includes a warm, humid rainy season and an intense dry season. The rainy season begins in April and ends in October. There is a brief interlude of harmattan occasioned by the northeast trade wind, with the main features being dust haze and dryness. This begins in November and lasts until January/February. The topography, high altitudes and undulating terrain of the FCT act as a moderating influence on the weather of the territory. Rainfall in the FCT reflects the territory's location on the windward side of the Jos Plateau and as a zone of rising air masses. The annual total rainfall is in the range of 1100–1600 mm.

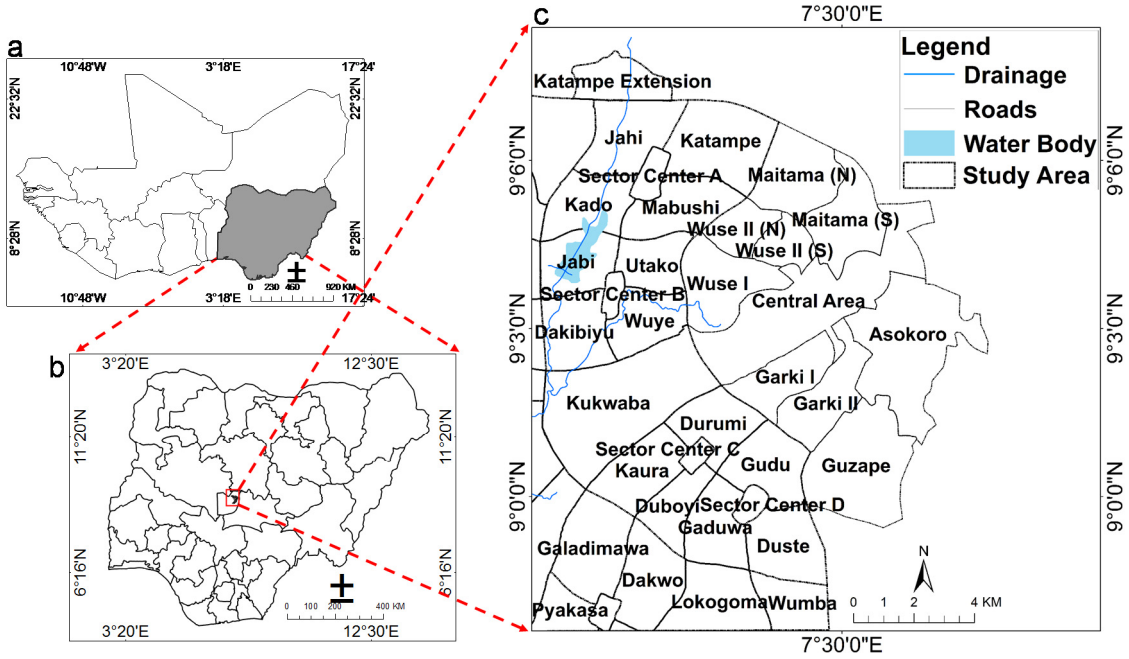

Figure 1. Location of study area. (**a**) West Africa inset Nigeria; (**b**) Nigeria inset Federal Capital City (FCT) and Abuja city in red rectangle and (**c**) Zoom of Abuja City showing major districts.

2.2. Data

In this current study, three epochs of cloud free Landsat series images were downloaded through the Earth Explorer web portal [41] for 1986, 2001 and 2014 at no cost (Table 2). Other ancillary datasets

used comprised of a hard copy of the Abuja Master Plan (AMP) obtained from the survey and mapping department of the federal capital development authority (FCDA) [42], a 20 m digital elevation model (DEM) purchased from the office of the surveyor general of the federation (OSGOF) [43], used for slope generation and GoogleEarth Maps [44]. The municipality administrative vector data was acquired from the National Space Research and Development Agency (NASRDA). Socioeconomic data such as census population was collected from the National Population Commission. Major road networks derived from a global position system field campaign in 2008 and a 2010 WorldView-2 very high resolution (VHR) satellite image were obtained from OSGOF.

Table 2. Satellite Image description.

Acquisition Date	Sensor	Spatial Resolution	Landsat Series	Number of Bands	Radiometric Resolution
26 December 1986	TM	30 m	Landsa 5	7	8 bits
27 December 2001	ETM+	30 m	Landsa 7	8	9 bits
7 December 2014	OLI-TIRS	30 m	Landsa 8	11	16 bits

TM: Thematic Mapper; ETM+ Enhanced Thematic Mapper Plus; OLI-TIRS Operational Land Imager-Thermal Infrared Sensor.

2.3. Overview of Methodology

The downloaded satellite images for this study were ortho-rectified/georeferenced L1T (terrain corrected) product from source. However, the geometric accuracy was verified by overlaying and comparing with existing maps. Here, coordinate system verification and projection to UTM zone 32, WGS1984, Minna Datum was ascertained. Radiometric correction was performed by converting the digital numbers (DN) to at-sensor radiance using the radiometric calibration module in ENVI-5 in conjunction with the provided metadata in the header file. The Flash Line-of-sight Atmospheric Analysis of Spectral Hypercubes (FLAASH) atmospheric correction in ENVI-5 was applied to the at-sensor radiance corrected images of 1986, 2001 and 2014 with the appropriate atmospheric and aerosol models (e.g., Kaufman Tenre aerosol retrieval, tropical setting and urban aerosol model) to produce atmospherically corrected at sensor reflectance images.

Basically, the SVM classifier was applied to the preprocessed multi-temporal epochs of Abuja for 1986, 2001 and 2014 to produce retrospective and recent LULC maps of the study area. The classified images were validated using the accuracy assessment measure based on reference points from multiple sources (e.g., pre-existing points, historical GoogleEarth maps and field campaigns. Subsequently, to determine and quantify LULCC amounts for the three time stamps considered in this study, a robust change detection approach for time t1 to detect what has been converted to another category in time t2 was explored. The transitions between t1 and t2 are presented as a change matrix which serves as the input to the proceeding step; mainly, the calibration and transition modelling of target LULC types. To derive relevant LULC information for city or municipality managers that could be used for settlement expansion analysis, qualitative and quantitative settlement expansion footprints and annual land-use change rate (ALUCR) were computed. In addition, driving forces analysis was conducted for modelling the transition between 1986 and 2001 and was subsequently used to test the predictive power of the LCM by producing a predicted LULC map for 2014. The real LULC map of 2014 was compared to the modelled LULC map predicted from the t1 and t2 categorical maps as a way of validating the LCM LULCC model. After validating the modelling step between 2001 and 2014, the model was considered fit for using a similar prediction timeframe (approximately 15 years) to predict the LULC scenario for 2050.

2.3.1. Production of LULC Maps and LULCC Detection

The LULC maps of 1986, 2001 and 2014 produced in this study were generated using the SVM-based classifier, and five major LULC classes were extracted (Table 3). To avoid the ”salt and

pepper or speckle effect" often associated with pixel based image classification, a post-classification step based on the majority/minority analysis approach was applied. The option of the 3 by 3 filtering kernel tool was chosen which is suitable for enhancing the quality of the produced maps as well as retaining the Minimum Map Unit (MMU) in urban studies such as the smaller features representative of the urban landscapes.

The LULCC detection was based on two main approaches: the first is the binary method that relays areas/information of change and no change. The output of this technique has only two options, it shows whether changes in pixels have occurred or not between two epochs [45]. A more detailed change detection technique is the post-classification comparison approach. This second method yields a "from-to" trajectory with an accompanying complete matrix containing records of exact count of transformed pixels from an initial class to another category [45]. However, the change or no-change detection method is often associated with the problem of precise threshold identification. The thresholding methods usually have external influences on the resulting differences and can be linked to atmospheric conditions (e.g., sun angle, variable soil moisture, phonological differences) coupled with the threshold which is subjective to the image scene and is somewhat dependent on analysis of the study area [45]. In the case of the post-classification method, autonomous image classification output is proceeded by applying a thematic overlay concept. This results in a complete "from-to" change matrix informative of transformations between categories of the multi-date maps [46]. This technique can be associated with high error propagation effects emanating from independent LULC maps. For instance, images of two dates with a classification accuracy of 80% is likely to have $0.80 \times 0.80 \times 100\% = 64\%$ combined classification accuracy [46]. The combination of the binary and post-classification change detection techniques yields a binary mask containing the extent of changed and unchanged areas at two time stamps [47]. The resultant change mask was subsequently overlaid on the second classified map which facilitates the identification of changed pixels at the t2 classified imagery [47]. In this current study, a hybrid approach which combines the change and no-change area binary maps of 1986–2001 and 2001–2014 derived from the Normalized Difference Vegetation Index (NDVI) was considered. Applying a NDVI thresholding approach directly for change detection underperformed in detecting many settlement and urban features, however, a direct image differencing approach by combining the near infrared difference with red difference performed better for urban change detection studies [48]. Consequently, an overlay of the areas of change was implemented to construct a change matrix of the study periods 1986–2001 and 2001–2014.

Table 3. Land cover classes used in the study.

Land Use/Cover	Types Description
Water	River, permanent open water, lakes, ponds and reservoirs
Built-Up	Residential, commercial and services, industrial, transportation, roads, mixed and other urban features
Vegetation	Coniferous and deciduous forest, mixed forest lands, shrubs and grassland (green areas)
Bare/Arable-land	Exposed soils, area of active excavation, Agricultural areas crop fields and fallow land
Complex Landscapes	Rock-outcrops metamorphosed rock dark soils, wetland and mucky water

2.3.2. Accuracy Assessment

Accuracy assessment was based on field reference data and an Orthophoto image from the survey and mapping department of FCDA for the 1986 image. The "Historical View" tool in Google Earth engine was used to validate the image from 2001. Field data, 2013 VHR and Google Earth images were used for the 2014 classification as reference. Given that the stratified random sampling approach employs the probability sampling design techniques which is key in demonstrating statistically rigorous assessment, for each of the produced LULC maps, a set stratified random points (200, 250 and 250 for 1986, 2001 and 2014, respectively) were generated using the random point tool in ArcGIS 10.1 toolbox (Table 4).

Table 4. Sample sizes allotted to the targeted LULC classes in 1986, 2001 and 2014.

LULC Category (Strata)	Sample Sizes			*Actual/Verified LULC Category*		
	1986	2001	2014	*1986*	*2001*	*2014*
Water	40	50	50	*40*	*50*	*50*
Built-Up	40	50	50	*38*	*50*	*45*
Vegetation	40	50	50	*55*	*52*	*55*
Bare/Arable-land	40	50	50	*41*	*59*	*56*
Complex Landscapes	40	50	50	*26*	*39*	*44*
Total column	200	250	250	*200*	*250*	*250*

The smoothed LULC maps were converted to polygons using the data conversion tool in ArcGIS 10.1. Subsequently, a column/field titled "Actual" was created for validating the classified map against the actual LULC. The randomly created points were used to verify the smoothed classified maps based on the reference data and actual LULC visualized from the reference data/VHR images (see italics row and columns in Table 4). The output matrices were further used to calculate overall, user's and producer's accuracies. The Kappa statistic, one of the commonly applied measures of difference between actual and change agreement, was computed [49].

2.3.3. Error Adjusted Area Assessment

In order to derive an error free area of LULCC information, the adjusted error matrix was computed. This involves three basic steps namely: (i) sampling design; (ii) response design and error adjusted area assessment (EAAA) analysis. The first step in EAAA is the sampling design stage. This is a practice used for determining the spatial unit subset that is subsequently used at the final EAAA step [50,51]. For these EAAA approaches, a collection of reference points were also based on the stratified random points to facilitate the computation of error adjusted change area detail as well as validate the SVM-based LULCC maps which requires a probability sampling approach [52]. This procedure allows the scientist to compute confidence interval estimates with statistical inferences and uncertainty measures.

Methodically, the five major LULC categories were used as sample strata. The LULC categories were suitable for stratification since they are the region of interest for communicating accuracy assessment results as well as the error adjusted class area estimates [50]. The stratified sampling is achievable by either equalizing the sample size of each class or making the sample size proportional to the target category spatial extent on the map. Equalizing the samples is more advantageous to the user's accuracy than the producer's and overall accuracies [53], whereas using the proportional sample size approach makes the standard errors of the estimated overall accuracies and producer's appear smaller in comparison with the equal sampling [50]. To robustly compute the EAAA, both sampling approaches were adopted, such as increasing the sample size of the target and s rear category such as built-up area in 1986 which conforms to Olofsson *et al.'s* [50] recommendation for obtaining good EAAA results.

The response design stage is the proceeding step used to compute the EAAA. It is a technique suitable for determining the sampling unit of reference data for LULC classification [53]. Accordingly, Table 4 was used for collecting the reference data showing the sample sizes and strata of LULC maps of 1986, 2001 and 2014. The final accuracy assessment analysis involves using the classified map containing m classes for constructing an error matrix [54]. Adopting the recommendation proposed by Olofsson *et al.* [50] for computing LULCC maps accuracies using stratified random sampling techniques in pixel-based classification maps, the area error inherent in the confusion matrices of the produced LULC classification and LULCC maps was adjusted for each category on the maps, while their area of proportions ($\hat{P}_{ij}$) was computed:

$$\hat{P}_{ij} = \mathrm{W}_i \frac{\mathrm{n}_{ij}}{n_{i+}} \tag{1}$$

where the area of proportion belonging to a category i in the map is W_i, while n_{ij} refers to the sample count labelled as i which belongs to class j contained in the reference dataset, the sample count mapped in category i is known as n_{i+} on the map. The adjusted error matrix of each cell element $\hat{P}_{ij}$ indicating the probability of a randomly determined area is classified to category i on the image data to class j in the reference data [55].

Using the newly computed error matrix, overall, user's and producer's accuracies were computed. The overall accuracy $(\hat{O})$ relays information on the overall proportion of correctly classified areas based on the sum of the diagonal adjusted error matrix represented as $\hat{P}_{ii}$.

$$\hat{O} = \sum_{i=1}^{m} \hat{P}_{ii} \tag{2}$$

The user's and producer's accuracies were computed based on Equations (3) and (4), respectively.

$$\hat{U}_i = \frac{\hat{P}_{ii}}{\hat{P}_{i+}} \tag{3}$$

$$\hat{P}_j = \frac{\hat{P}_{ij}}{\hat{P}_{+j}} \tag{4}$$

The user's accuracy for class i expressedãs $(\hat{U}_i)$ which is the proportion of area labelled as i having a class reference i, while producer's accuracy denoted as $(\hat{P}_j)$ of category j is proportional to the area of reference labelled j mapped as category j.

The area estimate and uncertainty were systematically computed using the approach proposed by Olofsson *et al.* [50], the constructed adjusted error matrix facilitated the computation of the area estimator using the area of proportion for category j. Here, the area of category j denoted as $(\hat{A}_j)$ was derived from Equation (5):

$$\hat{A}_j = A_{tot} \times \hat{P}_{+j} \tag{5}$$

A_{tot} refers to the total area, while Equation (6) serves as the area estimator embedded in an error adjusted estimator.

$$\hat{P}_{+j} = \sum_{i=1}^{m} \mathrm{W}_i \frac{\mathrm{n}_{ij}}{n_{i+}} \tag{6}$$

The area error adjusted estimator takes into account the area containing the error of omission present in the map category j and it eliminates the area of the map containing the error of commission [50]. The computed standard error $S(\hat{A}_j)$ was achieved based on Equation (7).

$$S(\hat{A}_j) = A_{tot} \times S\left(\hat{P}_{+j}\right) \tag{7}$$

Accordingly, the standard error computed for the stratified estimator based on the proportional area $S(\hat{P}_{+j})$ was derived from Equation (8).

$$\mathrm{S}\left(\hat{P}_{+j}\right) = \sqrt{\sum_{\mathrm{i}=1}^{\mathrm{m}} \frac{W_i \hat{P}_{ik} - \hat{P}_{ik}^2}{n_{i+} - 1}} \tag{8}$$

In order to assess uncertainty of the area estimates with sampling variability for computing confidence interval, the use of $\hat{P}_{+\ j}$ derived from the reference samples was considered rather than the $\hat{P}_{i+}$ from the map areas. Hence, $\hat{A}_j$ which is the approximate of 95% confidence interval (CI) was computed based on Equation (9).

$$CI = \hat{A}_j \pm z \times S(\hat{A}_j) \tag{9}$$

where z denotes the percentile of the standard normal distribution curve and 95% confidence correspond to z score of 1.96.

2.3.4. Land Use Change Analysis and Urban Growth Indicators

Information on land use change is vital, not only in spatio-temporal urban growth and transport analysis, but also in different global, regional, local and urban context analyses. The dynamics of urban areas such as the driving forces of urban development is reflected by land use change [56–58]. Hence, relevant indicators can be used as an effective means of quantifying and analyzing the spatio-temporal relationships between land use change and urban growth. In this study, one indicator was implemented to annualize the quantification of the spatio-temporal LULC change and urban expansion in Abuja. First, the so-called Annual Land Use Change Rate (ALUCR) was calculated, which was previously defined by Tian *et al.* [59] as follows:

$$\mathrm{ALUCR}_{a,t} = \frac{\left(\mathrm{LU}_{a,t} - \mathrm{LU}_{a,t-1}\right)/\mathrm{LU}_{a,t-1}}{\left(\mathrm{N}_t - \mathrm{N}_{t-1}\right)} \times 100 \quad (10)$$

where ALUCR_t (%) is the land use change rate; $\mathrm{LU}_{a,t}$ and $\mathrm{LU}_{a,t-1}$ are the total land area of land use class a in hectares at the time t (current year) and time $t-1$ (former year); N is the total number of years from time t (current year to time $t-1$ (former year)). In this way, ALUCR enables class-wise change analysis.

2.3.5. LULCC Model Implementation and Validation

The LCM analysis was implemented using the IDRISI Selva software. The modelling procedure involves change analysis, modelling transition potential and determination of driving forces, predicting change and validation of the model. The generated LULC maps of Abuja city for 1986, 2001 and 2014 met the minimum requirement for implementing the LCM change analysis and prediction in 2050. The LCM is a rigid model structure which is based on a fixed flow of procedure with a minimum requirement of two LULC maps and the initial map serves as t1 and later serves as t2. The 1986 and 2001 LULC maps were used for the change analysis step to assess changes between the two time stamps. The two dates had the same specification (matching backgrounds, legends and spatial characteristics) and were used as the basis for understanding the nature of change in Abuja. These maps were used to generate transition potential maps and the probability matrix which were suited for identifying prevalent transitions to the urban category and this, in turn, was used as an input for the modelling of land cover changes. In LCM analysis, the modelling transition potential is vital for change location determination [34]. The output of this step generates a series of transition potential maps that corresponds to significant land-cover transition into urban based on the change analysis phase implemented [34]. The transition maps must consider the suitability of image pixels that have transformed into urban pixels considering a number of driving forces or factors useful for modeling processes of historical change. In this study, elevation, slope and distance to existing urban forms in 1986 were used as predictive variables. The distance to urban areas was used in the modeling phase, while elevation and slope were used independently as have been considered in similar recent studies [29,60] which were documented to have influence on settlement expansion, urban growth or sprawl and were evident in the LULCC between 1986 and 2001. In 1986, the distance to urban areas was set as a dynamic factor for recalculating the prediction period of (14 years), from 2001 to 2014. As settlements expands, so does the distance to urban forms and this changes over time from 1986. To assess the influence of topography as a driving force, a spatial overlay of the urban footprint was performed on the slope layer. Likewise, randomly generated elevation points corresponding to settlement were extracted from the digital elevation model (DEM) and superimposed on the computed hill-shade as a backdrop layer.

The LCM also allows users to conduct a quick optional test of the potential exploratory model power for driving force which is presented in the Cramer's V. This depicts the correlation coefficient

indicating either no correlation (meaning a redundant variable) or perfect correlation referring to a significant potential variable ranging from 0.0 to 1.0, respectively [34]. Notably, the Cramer's V does not assure good model performance due to its lack of consideration of mathematical variables and their complex relationship [28], but it helps to determine the usefulness of a driving force [34]. In LCM, the MLP neural network is a feedforward neural one direction network that flows from an input to output with hidden layer(s) in between [61]. The computation of nodes can be grouped as layers where each node receives an input signal to the destination node [33]. For every input signal to another node, the subsequent layer contains the original input multiplied by a weighting and combined with a threshold which is channeled through the activation function in hidden linear or non-linear units [33]. The weights are defined in the training stage preceding the network prediction stage which uses a proportion of the data to change the weight in order to minimize errors in the observed and predicted outputs [33]. Generally, the MLP neural network is suitable for modelling multiple transitions at once [34], and was applied in this study.

The LCM prediction steps calculates the change rate from both the initial step and the transition potential maps generated from the second step in order to predict the future scenario of 2014. Based on the Markov-Chain analysis, implementing this step helps to ascertain the extent of transformation of other land-cover to urbanized areas in every transition that occurred in 2014 [34]. From this step, the hard and soft predictions are the two basic types of predictions derived as outputs [34]. The hard prediction result is the projected 2014 map showing pixels of the specific land-cover category which is the most likely class to be converted into. The soft prediction is to some extent a vulnerability map depicting pixels assigned to values ranging from 0.0 to 1.0, which is indicative of a pixel's probability to transform into an urban pixel in 2014 [34].

Model validation is an important step. In this study, validation was used to ascertain the quality of the predicted map of 2014 in comparison to actual 2014 LULC maps which is reality. Two notable approaches used in validating such models are the visual and statistical procedure [62]. Using the visual approach yields a crisscrossed tabulation between the 2001 LULC map, the predicted 2014 map and the 2014 actual map used for assessing the accuracy of the map model. The result of this process is a map containing four main categories [62], namely: (i) Hits which signify model prediction of change and that the situation actually occurred; (ii) False alarms that refer to the predicted change from one category to urban area with persistence in urban class; (iii) Misses suggest persistent model prediction that eventually changed to urban class in actual sense and (iv) Null success depicts areas where the model predicted no change and, indeed, no change occurred. The hits and null success are indicative of model correctness, while the false alarms and misses signify errors due to disagreement between the model simulation map and the reference map [62]. The figure of merit (FOM) is a ratio between hits, simulation hits, misses and false alarms and was computed to ascertain the overall agreement between the observed and predicted maps. FOM ranges from 0% signifying absence of overlap between the predicted and observed change, to 100% suggesting a perfect agreement between the predicted and observed change [63]. The statistical procedure measures the agreement between paired maps showing variable numbers of LULC categories [34]. The actual LULC map of 2014 is used as the reference map while the model simulation map was utilized for comparison. The kappa variation techniques were applied as the statistical validation procedure in this study. Here, the Kappa for no information (K_{no}) signifies overall accuracy obtained in the simulation run, while Kappa for location ($K_{location}$) means agreement level in a location [64]. Considering the difficulty in interpretation encountered with the Kappa for correctly assigned proportion against the proportion of incorrectly assigned by change ($K_{standard}$) [65], the $K_{standard}$ was not used in this study. However, $K_{location}$ was somewhat useful for the validation in the absence of $K_{standard}$ [66]. After assessing the model's predictive power, the model was applied to predict the LULC map of the 2050 scenario with the assumption of there being similar driving forces based on the changes between 1986 and 2014 LULC maps. Driving forces are not static, especially since the world is a dynamic system, so different triggers in variable rate and velocity are likely to evolve and may influence the urban evolution process as well as model results.

3. Results

3.1. Production of LULC Maps and Accuracy Assessment

Figure 2 presents the SVM-based LULC maps of Abuja city for 1986, 2001 and 2014. Five major classes, namely water, built-up, vegetation, bare/arable land and complex-landscapes were derived from the multi-date satellite images. It is apparent from Figure 2 that changes occurred in proportions of area covered by the retrospective LULC map categories, especially for built-up land which is the major focus of this study, and analyzing these patterns is useful for gaining insights about the composition of the total map area and changes in patterns during the considered years of analysis.

Table 5 presents the accuracy assessment obtained based on the pixel count error matrices from the LULC maps. The overall accuracies derived from the pixel count matrices of the generated retrospective LULC maps for 1986, 2001 and 2014 were 83%, 92% and 94%, respectively, while kappa accuracies were 81%, 93% and 94% in 1986, 2001 and 2014, respectively (Table 5).

To derive accurate proportions of the targeted LULC categories, the error adjusted area matrix (EAAM) computed based on the pixel count matrix was produced (Table 6). The EAAM gives more informative and accurate detail in terms of omission and commission errors leading to confusion and misclassification in the three LULC maps (Table 6). The robustness of the EAAM can be confirmed by comparing the overall accuracies derived from the pixel count with the one recorded from the EAAM.

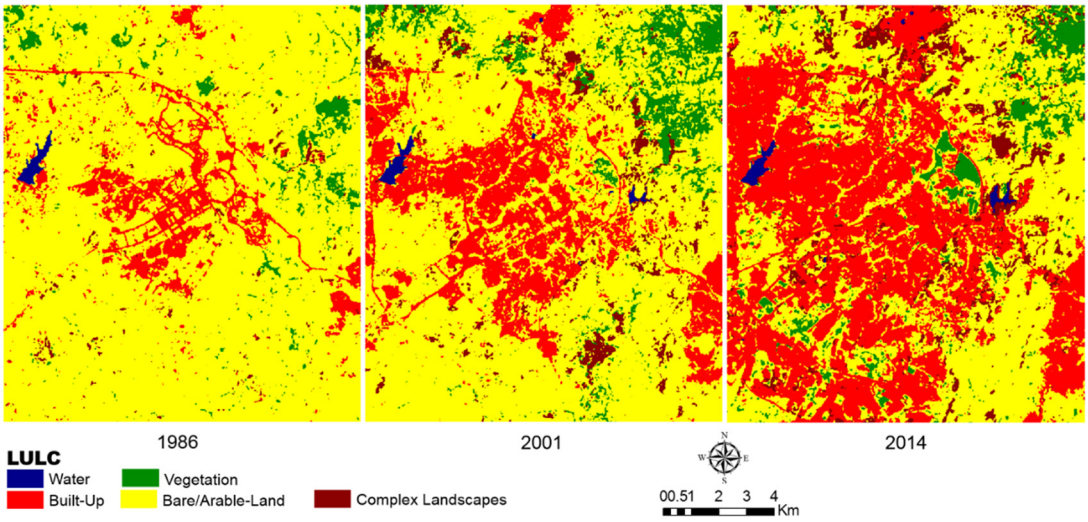

Figure 2. Classified images of Abuja for 1986 (**left**); 2001 (**middle**) and 2014 (**right**).

Table 5. Summary of Land Use Land Cover (LULC) map accuracies (%) for 1986, 2001, and 2014 based on the pixel count matrices.

Land Cover Class	1986		2001		2014	
	Producer's	User's	Producer's	User's	Producer's	User's
Water	100	100	100	100	100	100
Built-Up	94.7	92.3	96.0	96.0	100	88.2
Vegetation	72.7	100	94.2	96.1	90.9	100
Bare/Arable-land	65.9	65.9	78.0	92.0	82.1	92.0
Complex-Landscapes	84.6	55.0	94.9	75.5	100	89.8
Overall accuracy	83		92		94	
Kappa statistic	81		91		93	

The drop in the 1986 LULC map overall accuracy threshold of 83% based on pixel count to 69% using the EAAM is due to the inclusion of error of commission in estimating the proportion of area.

Similarly, a decline in the resultant pixel count overall accuracies was observed in the 2001 and 2014 LULC maps from 92% and 94% to 91% for both based on the EAAM (Table 6). Some confusion was observed between categories (e.g., BUP, VEG, BAL and CL). Major confusion occurred in the form of errors of commission given that incorrectly classified pixels are prominent in the rows, especially between BAL and CL in 1986 and 2001 (Table 6). Similarly, errors of omission are evident between VEG, BAL and CL in 1986 and 2001 (Table 6).

Table 6. Error adjusted matrix of LULC Maps of 1986, 2001 and 2014. WAT: Water; BUP: Built-Up; VEG: Vegetation; BAL: Bare/Arable Land; CL: Complex Landscapes.

Year	Class Name	WAT	BUP	VEG	BAL	CL	Total	User's (%)
1986	Water	0.390	0.000	0.000	0.000	0.000	0.390	100
	Built-Up	0.000	4.885	0.000	0.405	0.000	5.260	92
	Vegetation	0.000	0.000	5.060	0.000	0.000	5.060	100
	Bare/Arable-land	0.000	4.270	17.079	57.624	8.540	87.530	66
	Complex-Landscapes	0.000	0.000	0.308	0.484	0.968	1.760	55
	Total	0.39	9.13	22.45	58.53	9.51	100.00	
	Producer's(%)	100	53	23	98	10		69
2001	Water	0.520	0.000	0.000	0.000	0.000	0.520	100
	Built-Up	0.000	19.210	0.000	0.800	0.000	20.010	96
	Vegetation	0.000	0.000	22.463	0.458	0.458	23.380	96
	Bare/Arable-land	0.000	1.564	0.782	35.963	0.782	39.090	92
	Complex-Landscapes	0.000	0.000	0.694	3.471	12.844	17.010	76
	Total	0.52	20.77	23.94	40.69	14.08	100.00	
	Producer's(%)	100	92	94	88	91		91
2014	Water	0.640	0.000	0.000	0.000	0.000	0.640	100
	Built-Up	0.000	37.809	0.000	5.041	0.000	42.850	88
	Vegetation	0.000	0.000	5.550	0.000	0.000	5.550	100
	Bare/Arable-land	0.000	0.000	3.518	40.462	0.000	43.980	92
	Complex-Landscapes	0.000	0.000	0.142	0.570	6.268	6.980	90
	Total	0.64	37.81	9.21	46.07	6.27	100.00	
	Producer's(%)	100	100	60	88	100		91

3.2. LULCC Detection and Spatio-Temporal Analysis of LULC Distribution

The area distribution of the various LULC is reported in Tables 7–9 respectively. Comparing the pixel count matrices and the error adjusted matrix revealed a slight difference between the mapped and estimated area for the LULC categories. For all the categories, the produced maps fell within a 95% confidence interval of the estimated area which is indicative of the robustness and reliability of the produced maps [50].

The spatial arrangement of physiographic features was obtained by subjecting the classified images to spatial analysis, the information about changes in land cover proportion was derived. Subsequently, changes in the spatial composition of geographic features was obtained by comparing the classified images of 1986, 2001 and 2014 against each other (Table 10).

As displayed in Table 11, noticeable LULC changes appeared during the 28-year study timesteps. In this study, significant transitions from other classes into the water category were from vegetation and bare/arable land. During the 28 year time period, 0.03% of the vegetation transformed into water, as did 0.2% of bare/arable land. Approximately, 24.9% of bare/arable-land had been converted to built-up while 4.8% of area mapped as bare/arable-land in 1986 is now vegetation. Generally, persistence in all the classes stood at 4.3%.

Table 7. Proportion of LULC category for 1986.

LULC Types	Mapped Area (%)	Estimated Area (%)	Confidence Interval
Water	0.39	0.39	±0
Built-Up	5.26	9.13	±2.9
Vegetation	5.06	22.45	±5.4
Bare/Arable-land	87.53	58.53	±6.5
Complex-Landscapes	1.76	9.51	±4.1
Total	100.00	100.00	

Table 8. Proportion of LULC category for 2001.

LULC Types	Mapped Area (%)	Estimated Area (%)	Confidence Interval
Water	0.52	0.52	±0
Built-Up	20.01	22.77	±1.2
Vegetation	23.38	23.94	±1.1
Bare/Arable-land	39.09	40.69	±1.9
Complex-Landscapes	17.01	14.08	±1.3
Total	100.00	100.00	

Table 9. Proportion of LULC category for 2014.

LULC Types	Mapped Area (%)	Estimated Area (%)	Confidence Interval
Water	0.64	0.64	±0
Built-Up	42.85	37.81	±1.9
Vegetation	5.55	9.21	±1.7
Bare/Arable-land	43.98	46.07	±2.6
Complex-Landscapes	6.98	6.27	±0.3
Total	100.00	100.00	

Table 10. Spatial analysis result of error adjusted matrices of the 1986, 2001 and 2014 LULC maps from showing map category, class area in hectares and percentage and area changed in hectares.

Land Use Cover Types	1986		2001		1986–2001 Area Changed (ha)	2014		2001–2014 Area Changed (ha)	1986–2014 Area Changed (ha)
	Area (Ha)	%	Area (Ha)	%		Area (Ha)	%		
WAT	13,513.3	0.4	18,017.7	0.5	4504.4	22,175.6	0.6	4157.9	8662.4
BUP	316,180.7	9.1	719,778.9	20.8	403,598.3	1,310,053.1	37.8	590,274.1	993,872.4
VEG	777,775.9	22.4	829,479.7	23.9	51,703.8	319,150.4	9.2	−510,329.3	−458,625.5
BAL	2,028,040.6	58.5	1,409,643.6	40.7	−618,396.9	1,596,387.0	46.1	186,743.4	−431,653.6
CL	329,429.6	9.5	488,020.1	14.1	158,590.5	217,174.0	6.3	−270,846.1	−112,255.6
Total	3,464,940	100	3,464,940	100	3,464,940	100			

Table 11. Main LULC conversions from 1986 to 2014.

From Class	To Class	1986–2014 Area (ha)	1986–2014 Area (%)
Vegetation	Water	12.20	0.03
Bare/Arable-land	Water	65.80	0.20
	Built-Up	11,937.00	31.20
	Vegetation	1978.00	5.20
Persistence	(All classes)	18,137.10	47.40

3.3. Analysis of Settlement Expansion, Floodplain Encroachment and Driving Forces

The evolution of the built-up land category in Abuja city can also be seen in the LULC maps presented in Figure 2. From the time stamps, it was apparent built-up land increased by more than 50% from 1986 to 2001, and between 2001 and 2014, the expansion was approximately 48%, which is indicative of unprecedented urban growth and which conforms to the quantitative measures in Table 10.

For further spatio-temporal analysis, the overlay analysis of the extracted 2014 built-up time stamp onto the AMP map facilitated the evaluation of how settlement development did not conform to the plan. The AMP is a comprehensive document prepared to guide development in Abuja city to avoid chaotic urban development. From the overlay, a lateral settlement development situation was observed in Figure 3 and the uncontrolled lateral settlement expansion in Abuja suggests possible environmental challenges, such as floods due to floodplain encroachment, as highlighted with black boxes (Figure 3).

The computed annual land use change rate (ALUCR) analysis further established the LULC transformation rate in Abuja between 1986 and 2014 (Table 12). Built-up land being the core interest for Abuja city dramatically increased by 8.51% between 1986 and 2001 and by 6.31% from 2001 to 2014 (Figure 2 and Table 12).

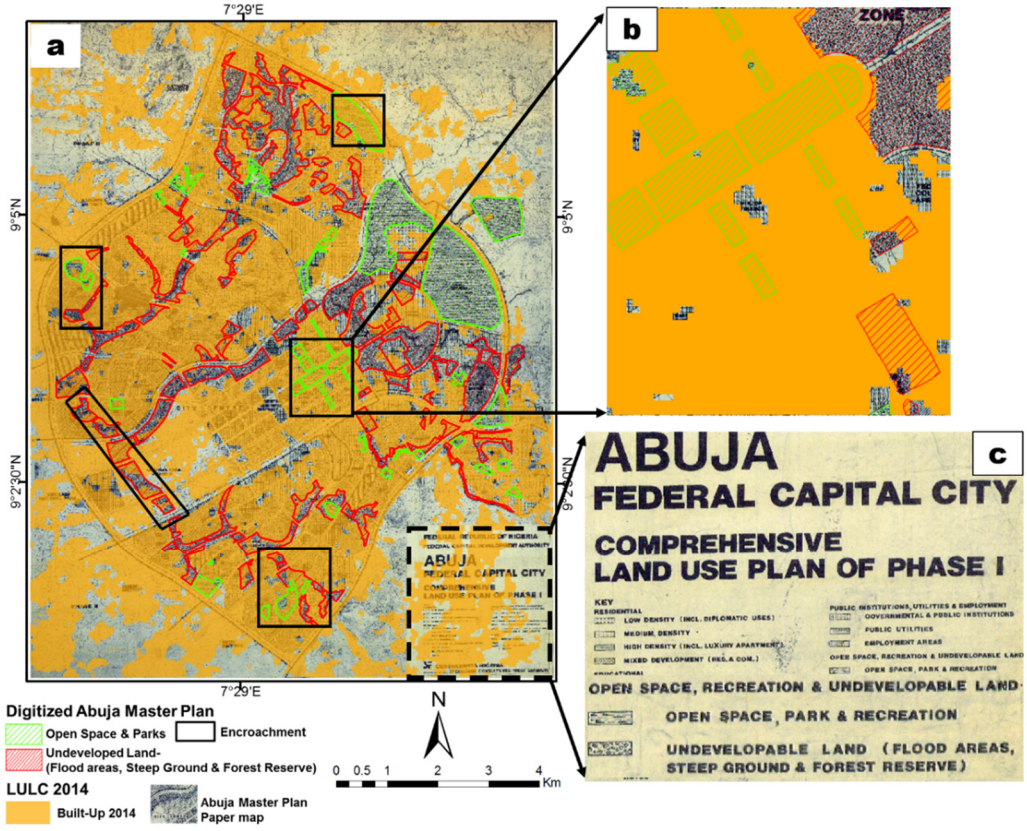

Figure 3. (**a**) Overlay of digitized open space and undevelopable area from the Abuja Master Plan (AMP) onto extracted 2014 built-up layer and AMP; (**b**) zoom-out of the overlay of digitized open space and undevelopable area from the AMP of Abuja for better visualization and (**c**) zoom of the AMP legend.

Table 12. Annual Land Use Change Rate (ALUCR) and use change in Abuja from 1986 to 2014.

Year	Water Area (ha)	LUCR %	Built-Up Area (ha)	LUCR %	Vegetation Area (ha)	LUCR %	Bare/Arable-land Area (ha)	LUCR %	Rock-Outcrop Area (ha)	LUCR %
1986	13,513.30	-	316,180.70	-	777,775.90	-	2,028,040.60	-	329,429.60	-
2001	18,017.70	2.22	719,778.90	8.51	829,479.70	0.44	1,409,643.60	−2.03	488,020.10	3.21
2014	22,175.60	1.78	1,310,053.10	6.31	319,150.40	−4.73	1,596,387.00	1.02	217,174.00	−4.27

The assessment of driving forces such as transportation infrastructure and suitable topography is presented in Figures 4 and 5 but is later discussed in Section 4.2.

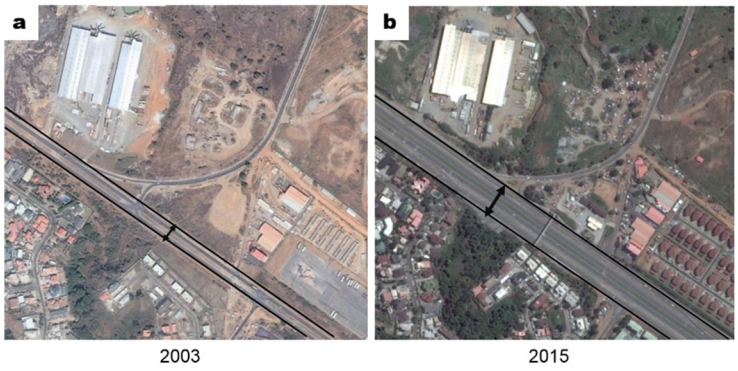

Figure 4. Example of the road expansion between 2003 (**a**) and 2015 (**b**) in the outer Northern Express Way of Abuja (image source Google Earth).

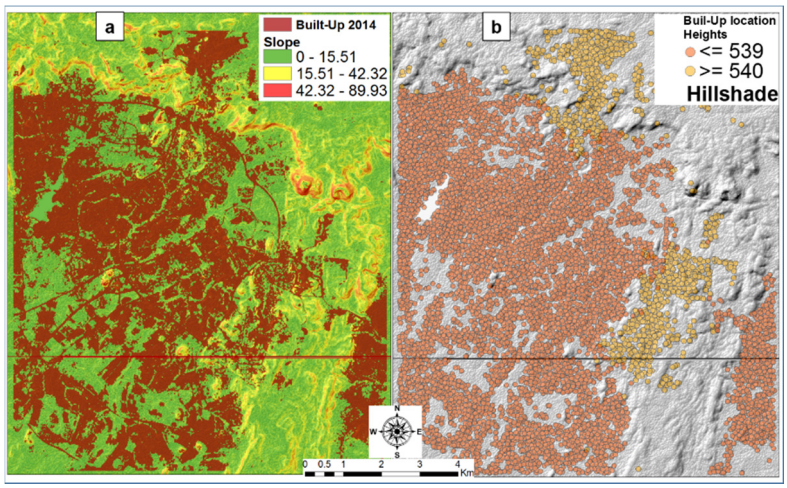

Figure 5. Assessment of the influence of topography on urban expansion. (**a**) Shows the GIS overlay of built-up on DEM derived slope. While (**b**) presents a constraint analysis showing built-up dependency on suitable heights as overlaid onto hillshade.

3.4. Land Use Change Model Implementation and Validation

Based on the LULCC maps, significant transitions occurred for all four categories: from water, vegetation, bare/arable-land and complex-landscape to built-up, hence, all were used as the major transitions in the model.

The transitions displayed varying urban spatial trends indicating that a divergent predictor variable will affect them. Table 13 presents the Cramer's V of the relevant and considered factors. It is a representation of the potential explanatory power of the major LULC category as a driving force in the settlement expansion process. The Cramer's V of 0.15 and above for any variable is useful, while values $\geqslant 0.4$ are good [34]. The proceeding step was to run the sub-model of relevant transitions and produce transition maps.

Table 13. Cramer's V driving force threshold for potential LULCC to built-up.

Driving Force	Cramer's V
Distance to Built-up in 1986	0.51
Bare/Arable Land	0.73
Vegetation	0.21

Figure 6 is a map illustration of the ocular validation of the projected urban LULCC of 2014 showing the precision achieved by the LCM model. Figure 7 depicts the validation map based on the crisscross which consists of hits, misses, false alarms and null success, with 1.08% hits achieved, 6.04% misses recorded, false alarms being 5.89% and null successes 86.99%.

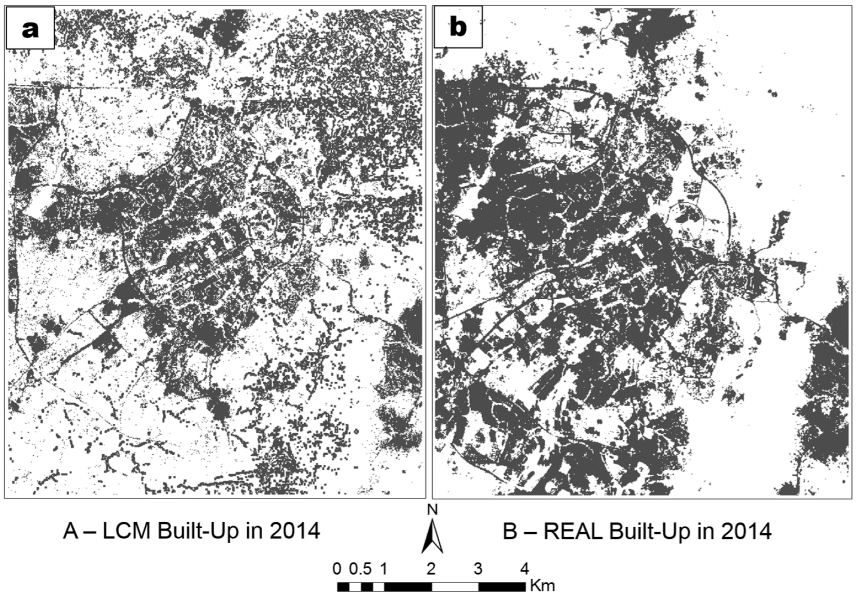

Figure 6. (**a**) LCM built-up; (**b**) Actual built-up footprint.

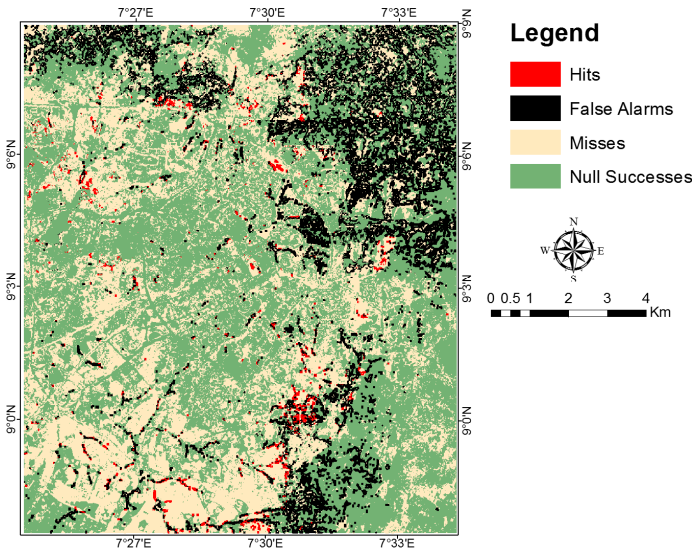

Figure 7. Ocular map validation of correctness using 2001 and 2014 as references and the projected LULC map for 2014.

Figure 8 presents the LULC projection into the year 2050 that was performed, similar to the model testing implemented between the 2001 and 2014 time stamps, the actual 2014 LULC map and built-up area expansion from 1986 to 2050.

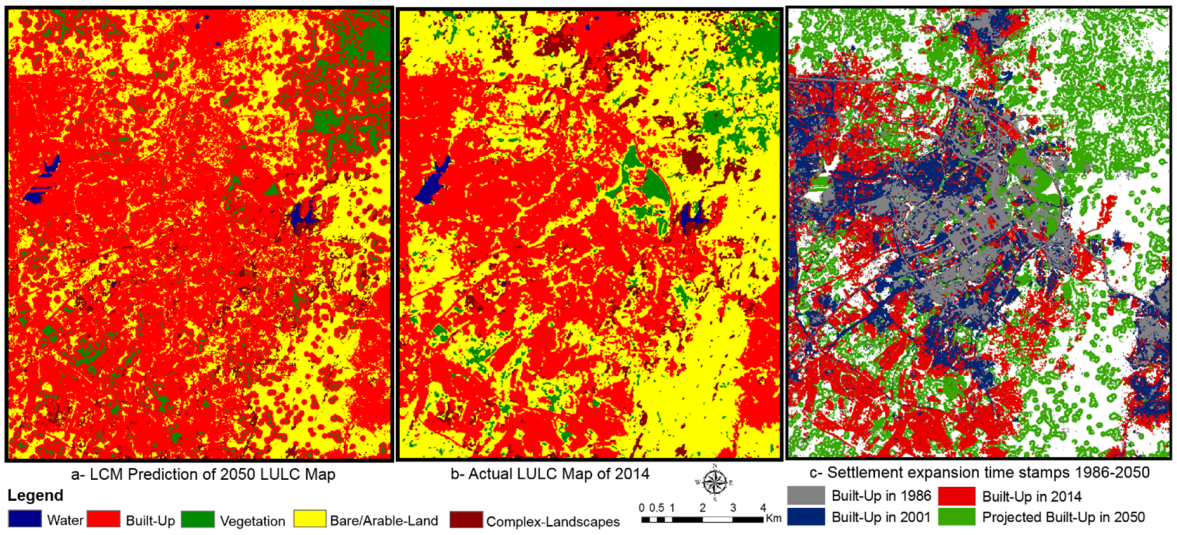

Figure 8. (**a**) Simulated LCM-based LULC map in 2050; (**b**) Actual 2014 LULC map; (**c**) Time stamps of built-up area from 1986 to 2050 projection scenario.

4. Discussion

4.1. Relevance of Data Adequacy for LULCC Mapping and Spatio-Temporal Analysis

Depending on the overall goal and context, target parameters, such as LULCC, could either be mapped or monitored, which is mostly dynamic and is best studied within a continuity framework. Given that LULCC can be linked to urbanization and global warming trends, adequate image time series are needed to identify changes and track trends from a historical perspective which is the basis for modelling the future. However, in tropical regions such as West Africa, especially Nigeria, cloud cover hampers the opportunity presented by the Landsat image archives to select the desired image time series from a particular Landsat sensor and, thus, leads to image scarcity. This challenge hindered LULCC analysis, such as of the settlement expansion and urbanization phenomena this study investigated. However, mapping and monitoring urbanization for analyzing imminent problems with limited data is still valuable for apt policy and decision-making, without which city managers would not be able to compare such empirical findings of urban development processes with other socio-economic indicators. Hence, due to the scarce availability of cloud free Landsat images for the same season over the study area, the authors adopted the multi-sensor and multi-temporal (MSMT) concept demonstrated in this study. However, this approach is associated with challenges that require thorough image pre-processing steps that must be fulfilled (see Section 2.3) since the direct application of Digital Numbers (DNs) will not suffice anymore in a MSMT context [67,68]. Therefore, conversion of DN to at-surface reflectance was performed to produce high quality scientific data for reliable downstream products such as the LULC maps. This procedure yields data that is illumination and atmospheric artefact independent and, therefore, plausible for making comparisons, such as in the change analysis performed in this study.

From the LULC change analysis of Abuja, it was found that water increased by 0.1% between 1986 and 2001 and, by 2014, another 0.1% increase was recorded. Generally, it is apparent that water surfaces expanded by 2% between 1986 and 2014 (Table 10). Substantial increase in the built-up class occurred between 1986 and 2001, by 403,598.3ha (20.8%), which is an average of more than 26,906 ha/year for the timeframe. Built-up area significantly expanded, by 590,274.1 ha (37.8%) from 2001 to 2014, which is more than 42,162.4 ha/year, with a net growth of approximately 993,872.4 ha in urban area in the study period (Table 10). A vegetation increase of 51,703.8 ha could be measured in 1986–2001 which is also apparent in Figure 2. However, between 2001 and 2014, vegetation declined drastically by 510,329.3 ha which can be linked to rapid deforestation, urban growth and a lack of parks and gardens.

The increase in vegetation in 1986–2001 can be attributed to annual variation (in 2001 comparatively high precipitation values were recorded) and increasing precipitation trends after the 1980 drought period. In addition to variability of natural conditions, the protection of green areas received more focus, which can be seen in the establishment of the millennium park and the developments of parks and gardens in the city center of Abuja.

Of the total change in built-up area, most of the areas were previously bare/arable land which formed the newly urbanized areas in the study period. Apparently, the dominant land use types in 1986 were natural vegetation cover and bare/arable land for cultivation, and the urban area (referred to as the built-up category herein) was found in the city center (Figure 2). The increments seen in the built-up category reveal rapid urban development was a result of the demand for residential, public offices, academic and business/commercial facilities. This is in line with the substantial growth witnessed in Abuja between 1986 and 2001, as highlighted in Table 10. From the classification results, it can be seen that urban expansion started to evolve in all directions (Figure 2). Noticeably, between 1986 and 2001 the observed decline in bare/arable land category by 17.8% is a significant change which can be attributed to the drought in the 1980s. Vegetation and complex landscape occupied 23.9% and 14.1%, respectively, of the study area in 2001, but this declined to 9.2% and 6.3% by 2014, respectively, due to both human and natural processes as well as misclassification errors. For instance, the complex landscape is a complicated category because, in this class, several activities are taking place, such as farming as well as quarrying in some locations. Similarly, landscapes such as murky water, dark soil and wetlands have identical spectral signatures and remain a source of misclassification in this study. Remarkably, the built-up category grew to 17% in the 2001–2014 study period. An explanation for the slight increase of (5.4%) bare/arable land can be linked to farmland expansion while the decline in vegetation may be attributed to intensified urban expansion in Abuja city.

4.2. Settlement Expansion, Floodplain Encroachment and Driving Force Analysis

With climate change impacts such as increased rainfall and decreased flood return period, encroached areas make buildings and people in such locations susceptible to flood impacts. Uncontrolled lateral expansion in Abuja also poses direct and indirect threats to essential ecosystems from a future settlement development perspective. According to Seto *et al* [69], in the coming decade, rapid land conversion is likely to occur in biodiversity hotspots, which in year 2000 were undisturbed. In the case of Abuja, urban growth was expected as there was provision for expansion in the master plan. However, according to FCDA [37], the actual land budgeted for specific purposes had been exceeded, and proximity to existing buildings or infrastructure is a factor that puts pressure on the available land irrespective of the land use specified for such parcels. Hence, for integrated spatial and socioeconomic analysis, the ALUCR can be compared with the population growth rate and other relevant indices for data driven decision making. The rapid growth in Abuja can be tied to population growth, construction of transportation infrastructure, business development and the government's development policies, such as massive housing estate development projects. Similarly, other potential social problems in Abuja due to rapid urban growth include the accelerated loss of highly productive farmlands, alteration of energy budgets with modifications to climatic, hydrologic, and biogeochemical cycles, habitat fragmentation or reduction in biodiversity [70]. Looking at the negative ALUCR of −4.73 between 2001 and 2014 for vegetation and the positive ALUCR of 1.02 between 2001 and 2014, this situation can be linked to micro-climate modifications such as urban heat island development in Abuja.

The observed LULC changes and settlement expansion in Abuja are driven by intertwined socioeconomic and environmental factors. Socioeconomically, some of the growth in Abuja can be associated with the oil boom and the relocation of government department headquarters to the center. During this period, a dramatic settlement expansion pattern was noticed which can be linked to the upward changing pattern of both the economy and the population. This was a period of rapid transportation infrastructure development in both the city and satellite towns (Figure 4). Two notable

patterns of expansion are outward growth of the city based on the master plan and sprawl development towards the satellite towns with a pattern discerned along the outer northern and southern expressways of the city.

Geographically, the spatial overlay of extracted built-up land for 2014 onto the slope map generated from a 20 m DEM proved that the built-up development pattern of Abuja city is supported by the suitable topography and slope of the converted landscape (Figure 5a). Results obtained from the overlaid 2014 LULC built-up footprint on DEM-derived hill-shade as the backdrop to Abuja city are presented in Figure 5b. The constrained analysis performed on built-up samples shows that significant urban expansion occurred in topographically flat and suitable landscapes of $\leqslant$539 meters (Figure 5b).

4.3. Land Use Change Model Implementation and Validation

The visual comparison presented in Figure 6 showed that the simulated 2014 built-up footprint performed satisfactorily. However, over prediction is apparent in the upper right corner of Figure 6a when compared to the actual data in Figure 6b which could be due to inadequacy of driving force restriction and model uncertainty. A 37.1% built-up extent in 2014 was achieved by the model prediction for the 2014 urban landscape, while the actual built-up extent in 2014 was 40.4%. A difference of 3.3% was observed, and this can be a source of the error found in the model. In this study, a FOM of 12.6% was achieved which can be regarded as a poor performance, however, it is still comparable with some recent studies such as by Olmedo [71] and Megahed [29] where FOM was 10.4% and 12.76%, respectively. This also suggests that, in modelling large areas such as Abuja, consideration of more complex predictive variables as driving forces will be needed to achieve better results. While visual assessment remains the swiftest approach to analyze spatial patterns, which is usually a weakness associated with the current statistical technique, ocular examination remains subjective and somewhat misleading. Hence, the current statistical technique is still vital in model validation [62]. The Kappa variation was used to compare the projected 2014 LULC map to the real LULC map of 2014 and realized a K_{no} of 85% and a $K_{location}$ of 95%. These high accuracy measures suggest that changes in the categorical maps are systematic for the 28 year (1986–2014) epoch assessed. It is also critical to carry out visual assessment throughout the FOM analysis because it helps the analyst identify localized areas of change rather than regions of no change [29].

The LCM prediction Figure 8a shows how built-up area will significantly grow and take over adjacent land categories in the absence of policies that ensure strict adherence to the master plan or sustainable spatial planning, in comparison to Figure 8b in the middle. This is indicative of continuous removal of natural cover as well as ecosystem destruction. Modification of natural cover such as vegetation will certainly reconfigure the energy balance (temperature development) such as the formation of an urban heat island (UHI) due to impervious surfaces, which has been established and well documented based on building configurations including shape, size, and geometry [11]. Therefore, the model result provides an insight into the need for a carbon mitigation strategy and green urban design in Abuja due to potential disappearance of vegetation cover. Also, Figure 8c illustrates the spatial pattern of built-up land in Abuja suggesting numerous environmental challenges (e.g., UHI potential, distortion of urban hydrology). Complementary to the UHI, urbanization can also influence precipitation patterns. In literature, two factors noted are: (i) the influence of urbanization in altering convective forces driving precipitation and; (ii) the variability of aerosol abundance in urbanized spaces [72]. Also, an observation of dedicated urban climate studies has been the occurrence of locational shifts and regional increases in convective precipitation linked to urbanization which thus results in an increase in surface temperature [73]. Thus, with the dozens of studies pointing to the impact of urbanization on precipitation, Abuja is unlikely to be an exception even though research outputs might differ if it is further explored.

4.4. Framework for Future Research

The absence of previous research on a city such as Abuja hampers opportunities for a comparison of the findings of this study regarding data selection, methodology used and results obtained. This study is just the tip of the iceberg. However, the research provides a sufficient basis for further studies, and, therefore, can be classified as foundation research that urgently needs to be followed-up with more integrated approaches that will address aspects this study did not consider. For instance, in accordance with numerous projections, rapid settlement expansion can be seen as unavoidable, especially considering the total world urban population is currently at approximately 7.4 billion, and by 2050, it is anticipated to range from 8.3 to 10.9 billion. In developing countries, 70%–80% of the population will be urban dwellers. As a result of this, urban planners proposed two coping strategies to address the ever-increasing population pressure exerted on urban areas. The first is through population control while the second put forwards the need for an efficient urban management agenda. The initial proposal has proven to be very challenging, especially in developing regions like West Africa, including Nigeria. Sustainable urban management is founded on two major planning processes, namely strategic and operational planning. In the case of urban planning, one of the principal datasets needed is land use. Fundamentally, land use data is useful for strategic and operational planning, particularly for detecting and monitoring changes, trends analysis and for future prediction based on scenarios/consequences and review of master plans. Therefore, a relevant aspect to be further investigated that is related to the generated dataset includes assessing the influence of settlement expansion on land surface temperature and UHI formation, flood risk zonation of the city and its integration with urban density information/urban structural types. This is integral to assessing risk and vulnerability to environmental phenomena such as climate change. It will also be worthwhile to compare the SVM based approached used in this study with other similar methods that have an integrated GIS approach with artificial neural network and fuzzy logic by incorporating additional driving force constraints based on additional data [32,74,75], and other tested integrated urban remote sensing and GIS approaches [76].

5. Conclusions

The FCC of Nigeria, Abuja, was used as the test site for this study using integrated remote sensing datasets and GIS modelling approaches. It was established that significant LULC change and settlement expansion has occurred. Due to the study timeframe and there being limited cloud free datasets available from a single Landsat sensor, the multi-sensor and multi-temporal images of Landsat (TM, ETM+ and OLI for 1986, 2001 and 2014) were used for this study. The utility of these datasets was realized through rigorous image pre-processing to ensure that real change over time was measured and the results obtained were reliable and fit for further use (e.g., informed policy and decision-making). Also, the application of a robust information extraction algorithm such as SVM required limited training samples and yielded good image classification. In future, the SVM and other advanced methods such as object oriented image analysis and random forest can either be integrated or compared to assess their performance in problematic or heterogeneous areas.

The core objective was to spatio-temporally analyze LULC for 1986, 2001 and 2014. Based on the pixel count error matrix, overall accuracies of the three LULC maps ranged from 82% to 94%. Contrary to these statistics, the adjusted area error gave a somewhat different accuracy measure that ranged from 69% to 91%. The study found that computing area information directly from pixel count for accuracy assessment can be misleading. Hence, in producing local maps that can be useful for evaluating the accuracy of global maps, climate modelling and other relevant applications, assessing error propagation in regional maps by applying the error adjusted area estimator yields a more reliable and informative result including confidence intervals and uncertainty measures. The different components of LULC change analysis allowed better understanding of the transformation processes, especially for the transition from the bare/arable land and vegetation categories to the built-up area class. The computed indices provided empirical insight into a realistic spatio-temporal situation,

and detailed annual land use and urban spatial expansion change rates in the study timeframe with major impacts on the landscape and potential influence on the local climate of Abuja. The forces governing such a momentous expansion might be numerous, however, apparent drivers in the case of Abuja included suitable topography, availability of public infrastructure, such as social amenities, and population growth, particularly in the past two decades.

Two salient aspects ascertained by this research are that massive impervious surface development is occurring due to urbanization, which may lead to elevated urban temperatures known as the UHI phenomenon. This phenomenon, is one of the likely climate control factors at a local scale highlighted by the Fifth Assessment Report of the IPCC [77], and COP 21 [78]. Complementary to the UHI is the change in drainage geography that may also increase surface runoff which translates to flash flood events in cities. With rapid urban expansion in Abuja, when rainfall increases, surface runoff is expected to increase and can trigger flash flood events in areas deficient of adequate drainage, especially looking at the 2050 built-up area projection in the context of climate change. From this study, further research is needed to empirically verify present and future impacts of urbanization on Abuja city.

Acknowledgments: This current research output forms part of a PhD Dissertation within the West African Science Service Center on Climate Change and Adapted Land Use (WASCAL) program on Climate Change and Land Use, which is funded by the German Federal Ministry of Education and Research (BMBF) and hosted by the Kwame Nkrumah University of Science and Technology, (KNUST), Kumasi. The publication was supported by the Open Access Publishing Found of the University Würzburg. Special appreciation is expressed to the Remote Sensing Unit at the Institute for Geography and Geology, University of Würzburg, (Germany) for the provision of research facilities.

Author Contributions: This research was conceptualized, written and revised by Mahmoud Ibrahim Mahmoud with contributions from all coauthors. Special thanks to Professor Christopher Conrad and Michael Thiel for methodological and technical contributions. The authors appreciate relevant comments and suggestions from all the reviewers that further improved the quality of the article.

Conflicts of Interest: The authors declare no conflict of interest.

References

1. Hahs, A.K.; McDonnell, M.J.; McCarthy, M.A.; Vesk, P.A.; Corlett, R.T. A global synthesis of plant extinction rates in urban areas. *Ecol. Lett.* **2009**, *12*, 1165–1173. [PubMed]
2. Yuan, F.; Sawaya, K.E.; Loeffelholz, B.C.; Bauer, M.E. Land cover classification and change analysis of the Twin Cities (Minnesota) metropolitan area by multi-temporal Landsat remote sensing. *Remote Sens. Environ.* **2005**, *98*, 317–328.
3. Lopez, E.; Bocco, G.; Mendoza, M.; Duhau, E. Predicting land cover and land use change in the urban fringe a case in Morelia City, Mexico. *Landsc. Urban. Plan.* **2001**, *55*, 271–285.
4. Seto, K.C.; Kaufmann, R.K.; Woodcock, C.E. Landsat reveals China's farmland reserves, but they're vanishing fast. *Nature* **2000**, *406*, 121–121. [CrossRef] [PubMed]
5. Turner, B.L.I. Local faces, global flows: The role of land use and land cover in global environmental change. *Land Degrad. Dev.* **1994**, *5*, 71–78. [CrossRef]
6. Grimm, N.B.; Faeth, S.H.; Golubiewski, N.E.; Redman, C.L.; Wu, J.G. Global change and the ecology of cities. *Science* **2008**, *319*, 756–760. [CrossRef] [PubMed]
7. Holdgate, M.W. The sustainable use of tourism: A key conservation issue. *Ambio* **1993**, *22*, 481–482.
8. World Health Organization. Urbanization: Urban Population Growth. Available online: http://www.who.int/gho/urban_health/situation_trends/urban_population_growth_text/en/ (acessed on 12 October 2015).
9. Taubenböck, H.; Wegmann, M.; Wurm, M.; Ullmann, T.; Dech, S. The Global trend of urbanization: spatiotemporal analysis of megacities using multi-temporal remote sensing, Landscape metrics, and gradient analysis. *SPIE Proc.* **2010**. [CrossRef]
10. UN Habitat. *Cities and Climate Change: Global Report on Human Settlements 2011*; UN Habitat: London, US, 2011.

11. Wentz, E.A.; Anderson, S.; Fragkias, M.; Netzband, M.; Mesev, V.; Myint, S.W.; Quattrochi, D.A.; Rahman, A.; Seto, K.C. Supporting global environmental change research: A review of trends and knowledge gaps in urban remote sensing. *Remote Sens.* **2014**, *6*, 3879–3905. [CrossRef]
12. Solecki, W.; Seto, K.C.; Marcotullio, P.J. It's time for an urbanization science. *Environ. Sci. Policy Sustain. Dev.* **2013**, *55*, 12–17. [CrossRef]
13. Stow, D.A.; Chen, D.M. Sensitivity of multi-temporal NOAA AVHRR data of an urbanizing region to land use/cover changes and misregistration. *Remote Sens. Environ.* **2002**, *80*, 297–307. [CrossRef]
14. Patino, J.E.; Duque, J.C. A review of regional science applications of satellite remote sensing in urban. Settings. *Comp. Environ. Urban Sys.* **2013**, *37*, 1–17. [CrossRef]
15. Rindfuss, R.R.; Stern, P.C. Linking remote sensing and social science: The need and the challenges. In *People and Pixels: Linking Remote Sensing and Social Science*; Liverman, D., Moran, E.F., Rindfuss, R.R., Stern, P.C., Eds.; National Academy Press: Washington, DC, USA, 1998; pp. 1–27.
16. Weng, Q. Global Urban monitoring and assessment through earth observation. In *Remote Sensing Applications*; Weng, Q., Ed.; CRC Press: Boca Raton, FL, USA, 2014.
17. Wentz, E.A.; Quattrochi, D.A.; Netzband, M.; Myint, S.W. Synthesizing urban remote sensing through application, scale, data and case studies. *Geocarto Int.* **2012**, *27*, 425–442. [CrossRef]
18. Hsu, C.W.; Lin, C.J. A comparison of methods for multiclass support vector machines. *IEEE Trans. Neural Netw.* **2002**, *13*, 415–425. [PubMed]
19. Mountrakis, G.; Jungho, I.; Ogole, C. Support vector machines in remote sensing: A review. *ISPRS J. Photogram. Remote Sens.* **2011**, *66*, 247–259. [CrossRef]
20. Tuia, D.; Pacifici, F.; Kanevski, M.; Emery, W.J. Classification of very high spatial resolution imagery using mathematical morphology and support vector machines. *IEEE Trans. Geosci. Remote Sens.* **2009**, *47*, 3866–3879. [CrossRef]
21. Sáez, J.A.; Galar, M.; Luengo, J.; Herrera, F. Tackling the problem of classification with noisy data using multiple classifier systems: Analysis of the performance and robustness. *Inf. Sci.* **2013**, *247*, 1–20. [CrossRef]
22. Verburg, P.H.; Kok, K.; Veldkamp, A. Pixels or agents? Modelling land-use and land-cover change. *IHDP Update* **2005**, *3*, 8–9.
23. Verburg, P.H.; Schulp, C.J.E.; Witte, N.; Veldkamp, A. Downscaling of land use change scenarios to assess the dynamics of European landscapes. *Agric. Ecosyst. Environ.* **2006**, *114*, 39–56. [CrossRef]
24. Verburg, P.H.; Schot, P.P.; Dijst, M.J.; Veldkamp, A. Land use change modelling: Current practice and research priorities. *Geo. J.* **2004**, *61*, 309–324. [CrossRef]
25. Brown, D.G.; Walker, R.; Manson, S.; Seto, K. Modeling land-use and land-cover change. In *Land Change Science*; Springer: Houten, The Netherlands, 2004; pp. 395–409.
26. Gong, W.; Li, Y.; Fan, W.; Stott, P. Analysis and simulation of land use spatial pattern in Harbin prefecture based on trajectories and cellular automata-Markov modelling. *Int. J. Appl. Earth Obs. Geoinfor.* **2015**, *34*, 207–216. [CrossRef]
27. Tayyebi, A.; Pijanowski, B.C. Modeling multiple land use changes using ANN, CART and MARS: Comparing tradeoffs in goodness of fit and explanatory power of data mining tools. *Int. J. Appl. Earth Obs. Geoinf.* **2014**, *28*, 102–116. [CrossRef]
28. Khoi, D.D.; Murayama, Y. Forecasting areas vulnerable to forest conversion in the Tam Dao National Park Region, Vietnam. *Remote Sens.* **2010**, *2*, 1249–1272. [CrossRef]
29. Megahed, Y.; Cabral, P.; Silva, J.; Caetano, M. Land cover mapping analysis and urban growth modelling using remote sensing techniques in Greater Cairo Region—Egypt. *ISPRS Int. J. Geo-Inf.* **2015**, *4*, 1750–1769. [CrossRef]
30. Hua, L.; Tang, L.; Cui, S.; Yin, K. Simulating urban growth using the Sleuth Model in a coastal peri-urban district in China. *Sustainability* **2014**, *6*, 3899–3914. [CrossRef]
31. Alsharif, A.A.A.; Pradhan, B. Urban sprawl analysis of tripoli Metropolitan City (Libya) using remote sensing data and multivariate logistic regression model. *J. Indian Soc. Remote Sens.* **2014**, *42*, 149–163. [CrossRef]
32. Grekousis, G.; Manetos, P.; Photis, Y.N. Modeling urban evolution using neural networks, fuzzy logic and GIS: The case of the Athens metropolitan area. *Cities* **2013**, *30*, 193–203. [CrossRef]
33. Sibanda, W.; Pretorius, P. Novel application of Multi-Layer Perceptrons (MLP) neural networks to model HIV in South Africa using Seroprevalence data from antenatal clinics. *Int. J. Comput. Appl.* **2011**, *35*, 26–31. [CrossRef]

34. Eastman, J.R. IDRISI Selva Tutorial. Available online: http://uhulag.mendelu.cz/files/pagesdata/eng/gis/idrisi_selva_tutorial.pdf 2014 (acessed on 10 December 2015).
35. Roy, H.G.; Dennis, M.F.; Emsellem, K. Predicting land cover change in a Mediterranean catchment at different time scales. In *Computational Science and Its Applications-ICCSA 2014*; Springer International Publishing: Guimarães, Portugal, 2014; pp. 315–330.
36. Vega, P.A.; Mas, J.F.; Zielinska, A.L. Comparing two approaches to land use/cover change modelling and their implications for the assessment of biodiversity loss in a deciduous tropical forest. *Environ. Model. Softw.* **2012**, *29*, 11–23. [CrossRef]
37. FCDA. The Review of abuja master plan. In Proceeding of the International Workshop for the Review of Abuja Master Plan, Ladi Kwali Conference Center, Sheraton Hotel, Abuja, Nigeria, 29 November–2 December 2001.
38. Aliyu, M.D.; Bashiru, S. Nigeria: Multiple forms Mobility Africa's Demographic Giant. Available online: http://www.migrationpolicy.org/article/nigeria-multiple-forms-mobility-africas-demographic-giant. (accessed on 2 April 2015).
39. UNFPA. Population Projection. UNFPA in Abuja 2015. Available online: https://data.un.org/CountryProfile.aspx?crName=NIGERIA (accessed on 27 March 2015).
40. Ujoh Mr, F.; Isa, D.; Olarewaju, O. Urban expansion and vegetal cover loss in and around Nigeria's Federal Capital City. *J. Ecol. Nat. Environ.* **2011**, *3*, 1–10.
41. EarthExplorer. 2014. Available online: http://earthexplorer.usgs.gov/ (accessed on 30 December 2014).
42. FCDA. *The Master Plan. for Abuja, in the New federal Capital City of Nigeria*; Federal Capital Development Authority Abuja: Abuja, Nigeria, 1979.
43. OSGOF. *20 m Digital Elevation Model. (DEM)*; OSGOF: Abuja, Nigeria, 2014.
44. Google Earth Maps. Available online: https://maps.google.com/ (accessed on 27 December 2014).
45. Weng, Q. Remote sensing image classification. In *Advances in Environmental Remote Sensing: Sensors, Algorithms, and Applications*; CRC Press: Boca Raton, FL, USA, 2011.
46. Singh, A. Digital change detection techniques using remotely-sensed data. *Int. J. Remote Sens.* **1989**, *10*, 989–1003. [CrossRef]
47. Mas, J.F. Monitoring land-cover changes: A comparison of change detection techniques. *Int. J. Remote Sens.* **1999**, *20*, 139–152. [CrossRef]
48. Veettil, B.K. A Comparative study of urban change detection techniques using high spatial resolution images. In Proceedings of the 4th GEOBIA, Rio de Janeiro, SP, Brazil, 7–9 May 2012.
49. Rosenfield, G.H.; Fitzpatirck-Lins, K. A coefficient of agreement as a measure of thematic classification accuracy. *Photogram. Eng. Remote Sens.* **1986**, *52*, 223–227.
50. Olofsson, P.; Foody, G.M.; Herold, M.; Stehman, S.V.; Woodcock, C.E.; Wulder, M.A. Good practices for assessing accuracy and estimating area of land change. *Remote Sens. Environ.* **2014**, *148*, 42–57. [CrossRef]
51. Stehman, S.V.; Czaplewski, R.L. Design and analysis for thematic map accuracy assessment: Fundamental principles. *Remote Sens. Environ.* **1998**, *64*, 331–344. [CrossRef]
52. Olofsson, P.; Foody, G.M.; Stehman, S.V.; Woodcock, C.E. Making better use of accuracy data in land change studies: Estimating accuracy and area and quantifying uncertainty using stratified estimation. *Remote Sens. Environ.* **2013**, *129*, 122–131. [CrossRef]
53. Stehman, S.V. Impact of sample size allocation when using stratified random sampling to estimate accuracy and area of land-cover change. *Remote Sens. Lett.* **2012**, *3*, 111–120. [CrossRef]
54. Congalton, R.G.; Green, K. *Assessing the Accuracy of Remotely Sensed Data: Principles and Practices*; CRC Press: London, UK, 2009.
55. Mas, J.F.; Pérez-Vega, A.; Ghilardi, A.; Martínez, S.; Loya-Carrillo, J.O.; Vega, E. A suite of tools for assessing thematic map accuracy. *Geogr. J.* **2014**. [CrossRef]
56. Aljoufie, M.; Zuidgeest, M.; Brussel, M.; van Maarseveen, M. Spatial–temporal analysis of urban growth and transportation in Jeddah City, Saudi Arabia. *Cities* **2013**, *31*, 57–68. [CrossRef]
57. Xie, Y.; Mei, Y.; Guangjin, T.; Xuerong, X. Socio-economic driving forces of arable land conversion: A case study of Wuxian City, China. *Glob. Environ. Chang.* **2005**, *15*, 238–252. [CrossRef]
58. Zhang, Y.; Guindon, B. Using satellite remote sensing to survey transportation-related urban sustainability. *Int. J. Appl. Earth Obs. Geoinf.* **2006**, *8*, 149–164. [CrossRef]

59. Tian, G.; Liu, J.J.; Xie, Y.; Yang, Z.; Zhuang, D.; Niu, Z. Analysis of spatio-temporal dynamic pattern and driving forces of urban land in China in 1990s using TM images and GIS. *Cities* **2005**, *22*, 400–410. [CrossRef]
60. de Noronha Vaz, E.; Caetano, M.; Nijkamp, P. Trapped between antiquity and urbanism-A multi-criteria assessment model of the Greater Cairo Metropolitan Area. *Land Use Sci.* **2011**, *6*, 283–299. [CrossRef]
61. Nazzal, J.M.; El-Emary, I.M.; Najim, S.A. Multilayer perceptron neural network (MLPs) for analyzing the properties of Jordan oil shale. *World Appl. Sci. J.* **2008**, *5*, 546–552.
62. Pontius, R.G., Jr.; Chen, H. *Land Change Modeling with GEOMOD*; Clark University: Worcester, MA, USA, 2006.
63. Rodríguez, N.E.; Armenteras-Pascual, D.; Alumbreros, J.R. Land use and land cover change in the Colombian Andes: Dynamics and future scenarios. *J. Land Use Sci.* **2013**, *8*, 154–174. [CrossRef]
64. Nadoushan, M.A.; Soffianian, A.; Alebrahim, A. Predicting urban expansion in Arak Metropolitan Area using two land change models. *World Appl. Sci. J.* **2012**, *18*, 1124–1132.
65. Kim, I.; Jeong, G.Y.; Park, S.; Tenhunen, J. Predicted land use change in the Soyang River Basin, South Korea. In Proceedings of the 2011 TERRECO Science Conference, Garmisch-Partenkirchen, Germany, 2–7 October 2011.
66. Pontius, R.G.; Millones, M. Death to Kappa: Birth of quantity disagreement and allocation disagreement for accuracy assessment. *Int. J. Remote Sens.* **2011**, *32*, 4407–4429. [CrossRef]
67. Chander, G.; Markham, B.L.; Helder, D.L. Summary of current radiometric calibration coefficients for Landsat MSS, TM, ETM+, and EO-1 ALI sensors. *Remote Sens. Environ.* **2009**, *113*, 893–903. [CrossRef]
68. Vicente-Serrano, S.M.; Pérez-Cabello, F.; Lasanta, T. Assessment of radiometric correction techniques in analyzing vegetation variability and change using time series of Landsat images. *Remote Sens. Environ.* **2008**, *112*, 3916–3934. [CrossRef]
69. Seto, K.C.; Güneralp, B.; Hutyra, L.R. Global forecasts of urban expansion to 2030 and direct impacts on biodiversity and carbon pools. *Proc. Natl. Acad. Sci. USA* **2012**, *109*, 16083–16088. [CrossRef] [PubMed]
70. Seto, K.C.; Fragkias, M.; Güneralp, B.; Reilly, M.K. A meta-analysis of global urban land expansion. *PLoS ONE* **2011**, *6*, E23777. [CrossRef] [PubMed]
71. Olmedo, M.T.C.; Paegelow, M.; Mas, J.F. Interest in intermediate soft-classified maps in land change model validation: Suitability *versus* transition potential. *Int. J. Geogr. Inf. Sci.* **2013**, *27*, 2343–2361. [CrossRef]
72. Rosenfeld, D.; Lensky, I.M. Satellite-based insights into precipitation formation processes in continental and maritime convective clouds. *Bull. Am. Meteorol. Soc.* **1998**, *79*, 2457–2476. [CrossRef]
73. Ashley, W.S.; Bentley, M.L.; Stallins, J.A. Urban induced thunderstorm modification in the Southeast United States. *Clim. Chang.* **2012**, *113*, 481–498. [CrossRef]
74. Riccioli, F.; El Asmar, T.; El Asmar, J.; Fagarazzi, C.; Casini, L. Artificial neural network for multifunctional areas. *Environ. Monit. Assess.* **2016**, *188*, 1–11. [CrossRef] [PubMed]
75. Triantakonstantis, D.; Stathakis, D. Urban growth prediction in Athens, Greece, using artificial neural networks. *Int. J. Civil. Struct. Constr. Archit. Eng.* **2015**, *9*, 193–197.
76. Mahboob, M.A.; Atif, I.; Iqbal, J. Remote sensing and GIS applications for assessment of urban sprawl in Karachi, Pakistan. *Sci. Technol. Dev.* **2015**, *34*, 179–188. [CrossRef]
77. IPCC. Climate change 2013. The physical science basis. Working group I contribution to the fifth assessment report of the intergovernmental panel on climate change-abstract for decision-makers. In *Groupe D'experts Intergouvernemental Sur L'evolution du Climat/Intergovernmental Panel on Climate Change-IPCC*; Stocker, T.F., Qin, D., Plattner, G., Tignor, M., Allen, S.K., Boschung, J., Nauels, A., Xia, Y., Bex, V., Midgley, P.M., Eds.; C/O World Meteorological Organization, 7bis Avenue de la Paix, CP 2300 CH-1211 Geneva 2 (Switzerland): Geneva, Switzerland, 2013.
78. COP 21. A Global agreement on the reduction of climate change. In *Paris Agreement under the United Nations Framework Convention on Climate Change*; UNFCCC: Paris, France, 2015.